Self-porating polymersomes of PEG–PLA and PEG–PCL: hydrolysis-triggered controlled release vesicles

Fariyal Ahmed, Dennis E. Discher *

Departments of Chemical–Biomolecular Engineering and Bioengineering, University of Pennsylvania, 112 Towne Building, Philadelphia, PA 19104, USA

Abstract

Controlled release polymer vesicles are prepared using hydrolysable diblock copolymers of polyethyleneglycol–poly-L-lactic acid (PEG–PLA) or polyethyleneglycol–polycaprolactone (PEG–PCL). Encapsulation studies with a common anti-cancer agent, doxorubicin, show loading comparable to liposomes. Rates of encapsulant release from the hydrolysable vesicles are accelerated with an increased proportion of PEG but are delayed with a more hydrophobic chain chemistry (i.e. PCL). Rates of release also rise linearly with the molar ratio of degradable copolymer blended into membranes of a non-degradable, PEG-based block copolymer (PEG–polybutadiene (PBD)). With all compositions, in both 100 nm and giant vesicles, the average release time (from hours to days) reflects a highly quantized process in which any given vesicle is either intact and retains its encapsulant, or is porated and slowly disintegrates. Poration occurs as the hydrophobic PLA or PCL block is hydrolytically scissioned, progressively generating an increasing number of pore-preferring copolymers in the membrane. Kinetics of this evolving detergent mechanism overlay the phase behavior of amphiphiles with transitions from membranes to micelles allowing controlled release.

© 2004 Elsevier B.V. All rights reserved.

Keywords: PEG–PLA; PEG–PCL; Hydrolytic degradation; Bilayer membranes; Micelles

1. Introduction

Lipid vesicles or liposomes have been widely investigated as encapsulators of hydrophilic drugs and proteins for several decades. Many if not all conventional liposome systems have proven to be both inherently leaky [1] and short-lived in the circulation [2]. Systems based on chemically active monomers, such as phospholipase sensitive [3,4] or ph/light desta-bilized [5–8] lipids, and polyethyleneglycol (PEG)–lipids [9–13] have been introduced as a means to control drug release. Chemically reactive polyethylene glycol PEG–lipids can play dual roles as liposome stabilizers that also, upon exposure to an environmental stimulus, effectively destabilize the carrier membrane via thiolytic [9,10] or hydrolytic [11–13] cleavage of their PEG–lipid bonds. As stabilizers, a small percentage (5–10%) of PEG–lipid was found, some time ago, to also delay liposome clearance [14]. In other words, PEG imparts stealthiness. Both ideas—controlled release and stealth—are extended here into

* Corresponding author. Tel.: +1-215-898-4809; fax: +1-215-573-6334.

E-mail address: discher@seas.upenn.edu (D.E. Discher).

purely synthetic polymer vesicle systems, which clearly offer broad control over vesicle properties.

The 'polymersomes' here are composed of block copolymers of both PEG and a hydrolytically susceptible polyester of either polylactic acid (PLA) or polycaprolactone (PCL). Both PLA [15–18] and PCL [19,20] have been widely studied as readily hydrolysable polyesters. PEG–PLA or PEG–PCL block copolymers have both been described before [21–26], and very recent illustrations of PEG–PLA vesicles [27–29] highlight the need for detailed characterization of release and degradability. Vesicle formulations of PEG–PLA or PEG–PCL with or without inert PEG–PBD (polybutadiene)—a well-documented vesicle former in water [30]—are shown here to provide programmed control over release kinetics. The dense 100% PEG corona of the PEG–PBD vesicles has recently been shown to deter membrane opsonization, and extend in vivo circulation times significantly beyond stealth liposomes [31]. While broader compatibility of PBD has been explored by others [32,33], the in vitro focus here is on the general principle of blending degradable and inert copolymers.

The elusiveness of making PEG–PLA vesicles is largely attributable to limited copolymer designs in relation to narrow requirements for a suitable lamellar phase. Extensive theoretical [34,35] as well as general experimental studies of block copolymer amphiphiles have established that aggregate morphology, in dilution, is principally determined by molecular geometry. Kinetic traps are many (e.g. entanglements, crystallization, or glassiness at high molecular weight, MW), but when solvated selectively, a delicate but now relatively well-understood balance of hydrophilic/hydrophobic segments emerges (Fig. 1A) [27,36]. This balance allows design of PEG-block based copolymers that—in the absence of degradation—form membranes in preference to other structures. Whereas diblock copolymers with small hydrophilic PEG fractions of $f_{EO} < 20\%$ and large MW hydrophobic blocks exhibit a strong propensity for sequestering their immobile hydrophobic blocks into solid-like particles (for PEG–PLA [21,26,37]), an increased $f_{EO} \sim 20–42\%$ generally shifts the assembly towards more fluid-like vesicles [27,28,30,38–43] or other "loose" micellar architectures [44–46]. For $f_{EO} > 42\%$, however, one generally finds both worm micelles (up to $\sim 50\%$
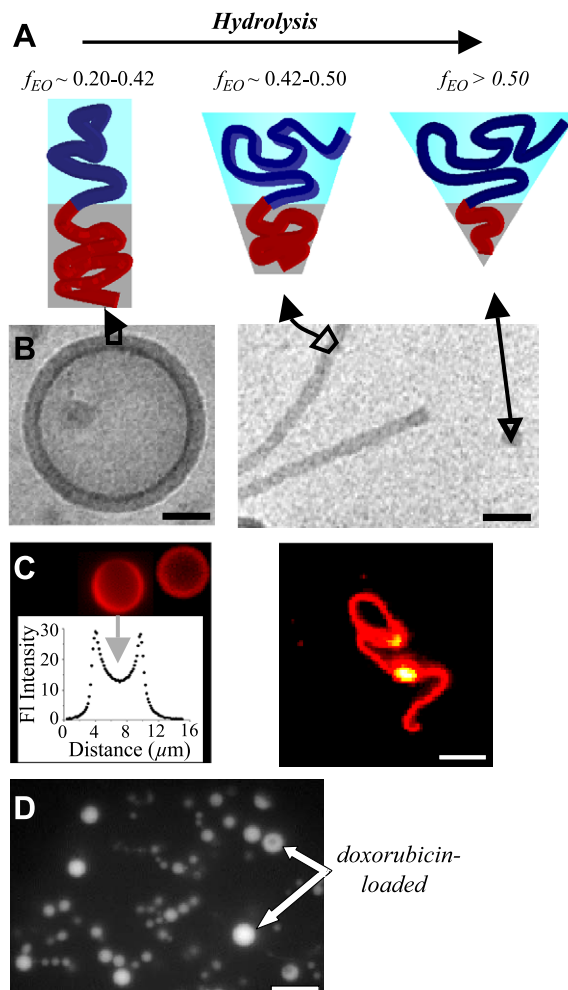

Fig. 1. Copolymer proportions, resulting architectures, and preliminary drug loading capabilities. (A) Illustration of diblock copolymer chains as a function of PEG (or PEO) volume fraction, f_{EO}. Increasing the f_{EO} fraction (e.g. degrading the length of the hydrophobic block) induces a molecular-scale transition: a bilayer forming copolymer ($f_{EO} \sim 0.25–0.42$) eventually transforms into a membrane-lytic cone-shaped detergent ($f_{EO} > 0.5$). (B) Cryo-TEM images of morphologies exhibited by diblock copolymers. Self-assembled vesicle of PEG–PLA diblock copolymer OL1, and several worm-like and spherical aggregates of the inert block copolymer of hydrogenated PEG–PBD [30]. Scale bar is ~ 20 nm. (C) Fluorescent images of giant architectures in dilute solution. The PLA block of OL1 is labeled, giving vesicles that are composed of fluorescently labeled OL1 blended with the unlabelled PEO–PBD copolymer, OB18. Intensity analysis (inset) of the fluorescent vesicles demonstrates edge brightness, and localization of OL1 in the vesicle membrane. At later times, blends also exhibit worm-like micelle morphologies. (D) Doxorubicin loaded vesicles imaged by fluorescence. Scale bars are 8 μm.

f_{EO}) [36,47,48] and, as noted by others, spherical micelles (for PEG–PLA [45,46,49], and PEG–PCL [50]). Lastly, although kinetic traps to equilibrium may deepen with MW, the equilibrium boundaries enumerated above between predominant microphases are only weakly dependent on MW. Recent work indeed shows that the aforementioned f_{EO}'s shift to lower values for diblocks only by about 5–6% per addition of 100 EO monomers [36].

The vesicle/micelle transitions outlined above would seem to provide a clear starting point for the design of novel copolymer carriers. While similar mechanisms have been exploited in otherwise conventional liposomal systems [8,51–53]. The kinetic aspects of phase transitions are not easily predicted but are of paramount importance when using 'active' chains such as the hydrolytically degradable PEG–PLA for release mechanisms. Considerable data in the literature indicate that degradation of PLA nanoparticles occurs on the order of weeks [15,44]. For the vesicles here, tunable, controlled release that ranges from hours to many days is demonstrated through copolymer blending within the membrane as well as polyester selection and chain architecture (i.e. f_{EO}).

2. Materials and methods

2.1. Copolymers and chemicals

The diblocks listed in Table 1, except for OB18 and OL1, were purchased from Polymer Source (Dorval, Quebec, Canada). Note that EO denotes ethylene oxide, and that polyethylene oxide is structurally the same as PEG. Tetramethylrhodamine-5-carbonylazide (TMRCA) was obtained from Molecular Probes (Eugene, OR). Dialysis tubing and dram vials were

purchased from Spectrum Laboratories (Rancho Dominguez, CA) and Fisher Scientific (Suwanee, GA), respectively. L-Lactide, mono-methoxy polyethylene glycol, tin ethyl hexanoate, toluene, chloroform, methylene chloride, sucrose, dextrose, phosphate buffer (PBS), doxorubicin, and fluorescent dextrans were all purchased from Sigma (St. Louis, MO).

2.2. Synthesis of the diblock copolymers

The PEG–PBD diblock (OB18) was synthesized by an anionic polymerization technique described elsewhere [54]. Diblock copolymers, listed in Table 1, were synthesized by standard ring opening polymerization detailed below for the PEG–PLA diblock, OL1. Briefly, OL1 used L-lactide and methoxy polyethylene glycol, which were pre-purified by recrystallization from ethyl acetate and toluene, respectively. The catalyst, tin ethyl hexanoate was used without further purification. All the reagents were dissolved in toluene solvent and placed in a sealed pressure tube under argon atmosphere, due to the sensitivity of the lactide monomer to degradation. The reaction vessel was placed in an oil bath at 100 °C, and polymerization was allowed to proceed for 2 h. Polymerization was terminated with a 10-fold excess of hydrochloric acid, and the polymer was further washed in ice-cold cyclohexane. The final product was subsequently lyophilized into a white powder and, when needed, solubilized in chloroform. ^{1}H NMR was used to determine the number of monomer units in each block. Gel permeation chromatography was used to determine the total number-average molecular weights, M_n, as well as the polydispersity indices (P.D.). Moreover, preliminary separations after base-catalyzed hydrolysis (pH>12) demonstrated that these synthetic diblocks undergo complete degradation in ≤24 h. The PEG volume fraction (f_{EO}) was converted from the measured mass fractions by using homopolymer melt densities: 1.13, 1.09, 1.14, and 1.06 g/cm^3 of PEG, PLA, PCL, and PBD, respectively.

2.3. Characterization of OL1 vesicles

Vesicles of pure OL1 block copolymer were prepared by dissolving polymer at 1 wt.% in water. The solution was stirred for at least 6 h at room temperature and OL1 vesicles were observed by cryogenic

Table 1
Physical properties of the various diblock copolymers

Copolymer name	Formula $A_m - B_n$	M_h[a] (kg/mol)	M_n (kg/mol)	P.D.	f_{EO}
OL1	$EO_{43} - LA_{44}$	3.2	6.0	1.1	0.33
OL2	$EO_{109} - LA_{56}$	4.0	10.0	1.16	0.49
OCL1	$EO_{46} - CL_{24}$	2.7	4.77	1.19	0.42
OCL2	$EO_{114} - CL_{114}$	12.9	18.0	1.50	0.28
OB18	$EO_{80} - BD_{125}$	6.8	10.4	1.1	0.29

[a] $M_h \sim n \times M_{monomer}$.

transmission electron microscopy (cryo-TEM) [55]. Briefly, samples of the polymer solution were immersed in a microperforated grid under controlled temperature and humidity conditions. The assembly was then rapidly vitrified with liquid ethane, and kept under liquid nitrogen until loaded onto a cryogenic sample holder. Images (Fig. 1B) were obtained with a JEOL 1210 TEM at 120 kV using a magnification of 20,000 along with a nominal under focus for improved resolution and digital recording.

2.4. Labeling of PEG–PLA (OL1) block copolymer

Since the PEG block of the OL1 and OL2 block copolymer was protected with a methoxy group, only the hydroxyl end group of the PLA block was susceptible to modification with tetramethyl rhodamine-5 carbonyl azide (TMRCA; MW 455.5 Da). The modification involves TMRCA conversion to an isocyanate, which then modifies the hydroxyl end group to a urethane. This end-group modification using a 1:1 polymer to dye mole ratio was carried out overnight in a mixture of toluene and methylene chloride (2:1 v/v) at 60 °C. The reaction was carried out in an organic phase primarily to minimize hydrolysis of the PLA block. Excess, unreacted TMRCA dye was dialyzed (MWCO 3500) into chloroform for 1 week, and the labeled block copolymer was stored at 4 °C.

2.5. Preparation of polymer bilayers and encapsulant loading

Polymer blends with OB18 and either OL or OCL block copolymer were prepared by first solubilizing the polymers at desired molar ratios in chloroform. The organic solvent was then evaporated under nitrogen, followed by vacuum drying for 7 h to remove trace amounts of chloroform as the polymer film dried onto the glass wall of a dram vial. The film was subsequently hydrated with solutions of hydrophilic encapsulants such as sucrose, fluorescently tagged dextrans, or ammonium sulfate (for subsequent doxorubicin loading, below). Upon hydration, vesicle self-assembly was further promoted in a 60 °C oven for ∼ 12 h.

Doxorubicin loading was achieved after vesicle formation by a variation of the ammonium sulfate-driven permeation method of Barenholz et al. [56]. Unencapsulated ammonium sulfate was removed by dialysis (cutoff 3.5 kDa) into isotonic PBS. The drug was added to the vesicle suspension with membrane permeation and accumulation promoted by the species gradients between inside and out of the vesicles. A 10-h incubation at 37 °C followed by 10-h dialysis into PBS proved sufficient for doxorubicin loading based on both fluorescence microscopy and spectrofluorimetry.

2.6. Vesicle isolation and NMR analysis

Polymer films of pure OB18, OL2, and OL2/OB18 at 50:50 blend ratio were prepared as above, using deuterated water (D_2O). Vesicle blends were separated from free monomers and other small aggregates by extensive dialysis (cut-off ∼ 1 MDa). Post-dialysis, the polymer solution was thoroughly dried using a rotavap. Pure and 50:50 blend films were subsequently dissolved in $CDCl_3$ for room temperature ^1H NMR analysis (Astra500 spectrometer, 500 MHz).

2.7. In vitro release kinetics

Micron-sized vesicles loaded with hydrophilic encapsulants were suspended in PBS (pH 7.0; 300 mosM) and incubated in a closed chamber formed with a gasket seal between a bottom cover slip and a top glass slide (height ∼ 100 μm). Vesicles were imaged with either bright field or phase contrast using a Nikon TE-300 inverted microscope. Phase contrast microscopy was possible based on differences in the refractive indices of the encapsulant and external buffer solution (e.g. sucrose inside and PBS outside). In vitro release kinetics was monitored over time by quantifying the population of vesicles that either retained ("loaded") or released ("empty") lumenal encapsulants. An average of 150–300 giant vesicles of various sizes was monitored over the time course of the experiment.

3. Results

3.1. PEG–PLA vesicles and blends

Both PLA and PCL are generally considered hydrophobic provided they are of sufficiently high molecular weight [27]. The spontaneous aggregation and assembly of OL1 copolymer (Table 1: EO_{43}–

LA$_{44}$) into lamellar or bilayer morphology—i.e. a vesicle—in dilute solution is verified by direct cryo-TEM imaging (Fig. 1B). The hydrophobic core of the membrane provides the contrast and has a measured width $d \approx 10.4 \pm 1.4$ nm.

The miscibility of OL1 block copolymer in a vesicle membrane with OB18 (Table 1: EO$_{80}$–BD$_{125}$) is demonstrated in Fig. 1C by fluorescence microscopy on 'giant' vesicles. The hydroxyl end group of the hydrophobic PLA block was first reacted with fluorophore (TMRCA), and the labeled copolymer was then blended in a good solvent with both unlabeled OL1 and OB18 block copolymer at molar ratios of 5:20:75, respectively. Subsequent preparation of a dried film of this blend followed by overnight hydration lead to spontaneous, self-directed assembly of polymersomes that were many microns in diameter. Giant vesicles show similar levels of fluorophore partitioned into the edge-bright membranes (see inset intensity analysis). A more quantitative analysis of miscibility is provided in the following section.

In addition, osmotically driven shape and volume changes of such giant vesicles [30] allow visual proof that water necessarily permeates the membrane, which is a pre-requisite for hydrolytic cleavage.

Fig. 1D shows OL1 vesicles stably containing doxorubicin—a widely used anti-tumor therapeutic [57–59]. The result illustrates both the initial integrity and the loading capabilities of the vesicle membranes. The increased membrane thickness of the polymersomes is probably responsible for two to three times longer loading times. Nonetheless, doxorubicin loading proves similar to liposomes [56] with roughly 1:1 copolymer: drug (mol/mol) ratios as estimated by spectrofluorimetry. The following sections focus on the encapsulant release of model hydrophilic drugs ranging in molecular weights from $\sim 10^2$ Da (like doxorubicin) to 10^5 Da.

3.2. Miscibility of PEO–PLA in PEO–PBD

To address block copolymer miscibility in lamellar architectures such as bilayer vesicles, blends of OL2/OB18 were prepared with fluorescently tagged, TMRCA-OL2 (Fig. 2). To remain within the quenching limit of the fluorophore, varying amounts of TMRCA-OL2 were added to a constant OL2/OB18 blend ratio of 50:50 mol% (Fig. 2A). The fluorescent

intensity of the vesicle membrane increases linearly with the added TMRCA-OL2 polymer. Since 4% labeled OL2 provided an adequate signal, it was introduced at this percentage to unlabeled OL2 for blending with OB18 from 5 to 100 mol%.

Upon hydration and self-assembly, vesicle populations were imaged under set conditions of dilution and
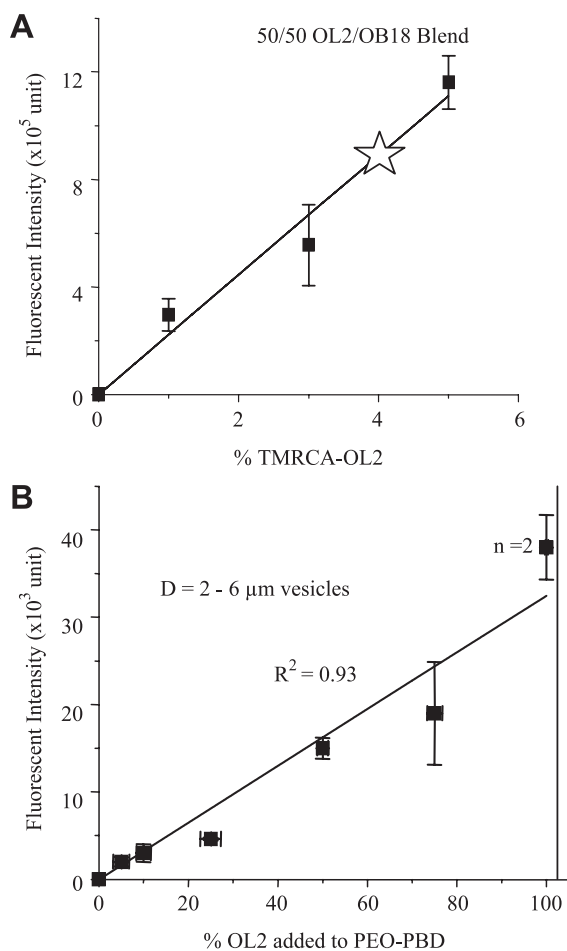

Fig. 2. Block copolymer blend miscibility in giant vesicles. (A) Proportional increase in membrane fluorescence with increased mol% of fluorescent TMRCA-OL2 in a blended polymersome membrane. Based on the strong intensity with 4 mol% (white star) of fluorescent OL2, this mol% was used in all further studies of blends. (B) Proportional increase of membrane fluorescence intensity with increasing OL2 (total) in OL2/OB18 blended polymersomes. In either panel, $n \geq 10$ vesicles (unless indicated) of diameter $2-6$ μm were analyzed by fluorescence microscopy under conditions of constant dilution (1:50), and fixed camera gain and exposure time.

image collection. Peak or edge intensities of the vesicle membranes were averaged over vesicle diameters ranging from 2 to 6 μm. These intensities appeared to be consistent and reproducible for three independent samples prepared over several weeks, implying stability of the fluorophore conjugate. The clear linear trend shows that increasing amounts of blended OL2 give a proportional increase in the intensities of the polymersome membrane.

As a check on the fluorescence imaging results, NMR was done on blended vesicles made with 50:50 OL2/OB18. Analysis of the pure OL2 and OB18 spectra showed the respective peaks for PLA, PEG and PBD, PEG [25,60–63]. The nominal 50:50 OL2/OB18 blend appeared to be a summation of the two individual spectra. The mol% OB18 in the blend was derived from the decrease in the integrated intensity ratio normalized to PEG, using the high-ppm OB18 peak in the pure sample [($\delta_{PBD,-CH=}$=5.29 ppm: $I_{5.29ppm}$=0.51), ($\delta_{PEG,CH2}$=3.64 ppm: $I_{3.64ppm}$=1.0)] vs. the blend sample [($\delta_{PBD,-CH=}$=5.15 ppm: $I_{5.15ppm}$=0.24), ($\delta_{PEG,CH2}$=3.68 ppm: $I_{3.68 ppm}$=1.0)]. The high ppm peak thus had a relative integrated intensity of 0.51 that decreased to 0.24 for the nominal "50:50 blend". The decrease is due to the PEG contribution from OL2. Accounting for the different PEG chain length allows a straightforward determination of the actual blend ratio as (OL2/OB18)=44:56 mol% (from NMR). Similar analyses of other resonant peaks (e.g. $\delta_{PBD,=CH2}$=4.91 ppm) suggest an error of about 7%. To summarize, the linear increase of fluorescence intensities with OL2 blend ratios (Fig. 2) along with the appearance and quantitation of characteristic NMR peaks for both copolymers in OL2/OB18 blends provides clear evidence of OL miscibility in OB18 blends.

Fig. 3. Release from polymer vesicles. (A) Phase contrast microscopy images of degradable polymersome carriers in a sealed chamber. Vesicles of 25 mol% blends of OL1 in OB18 are loaded with sucrose (300 mosM) and suspended in an isotonic buffer. The vesicles are initially dense and phase dark (i). Over time (~h), vesicles become phase light—losing their encapsulant—and rise to the top of the chamber (ii). Over longer times (~days), vesicles exhibit altered morphology and finally disintegrate (iii). (B) Histograms of "loaded" and "empty" vesicles evolve dramatically over the time course of the experiment. At initial times, the distribution is dominated by encapsulant "loaded" carriers (~90%). After 4 days, dominant fractions (~80%) of the visible vesicles appear "empty". Scale bars are 5 μm.

3.3. Visualizing hydrophilic encapsulant release

Blends of OL1 or the other degradable diblocks (Table 1) with the inert copolymer OB18 prove particularly useful in protracting the time scales for observation of membrane transformation and release
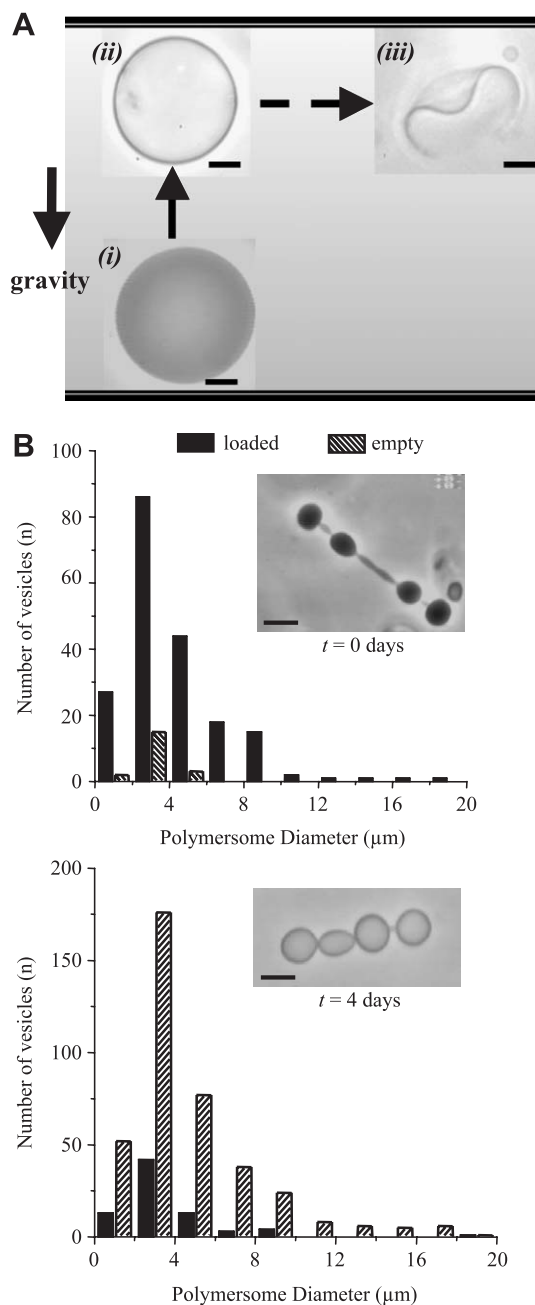
processes. For a given blend ratio, vesicles were made in sucrose (see Materials and methods)—a prototypical low molecular weight encapsulant. When diluted into PBS and added to a 100-μm-high sealed chamber for long-term microscopy, vesicles initially settle and appear dark under phase contrast microscopy (Fig. 3A(i)). This is due to differences in both the specific gravity and the refractive index of the sucrose encapsulant as compared to the external PBS. Over a span of hours to days in the sealed chamber, a given vesicle will become phase light, buoyant, and rise to the top of the chamber (Fig. 3A(ii)). Few, if any, vesicles are seen as either half-dark or halfway above the bottom, implying a two-state system with respect to encapsulant retention, i.e. loaded or ''empty''. At longer times, the empty vesicles, at the top of the chamber, lose their morphology and begin to clearly disintegrate in solution (Fig. 3A(iii)). In contrast, pure OB18 vesicles show essentially no loss of encapsulant over the duration of the study, fully consistent with previous measures of polymersome stability [64].

Histograms of phase contrast vesicles for a given sealed chamber are binned by vesicle size (Fig. 3B), and show clear population shifts from loaded to empty vesicles over hours to days of periodic observation. Since vesicle numbers in all size bins (from 2 to 20 μm) change dramatically over time, the histograms indicate no strong dependence on vesicle diameter. This suggests a surface 'erosion' mechanism that occurs locally in the membrane as opposed to a faster process with total degradable mass (which scales as $\sim R_{ves}^2$). The release studies outlined below demonstrate erosion as a clear poration process with an initial, characteristic pore size.

3.4. Growth of membrane pores of finite size

In visually monitoring release from micron-sized vesicles (Fig. 3A(ii)), it is clear that these vesicles retain their overall morphology after releasing their encapsulant. Hydrolysis of the PLA chains in the hydrophobic core of the bilayer is likely to generate some curvature-preferring chains (with $f_{EO}=0.42$), which localize and induce the growth of pores in the membrane. In order to verify pore induction in the vesicle membrane and provide a gauge for pore size, kinetically tractable 25:75 blends (OL1/OB18) were used for monitoring release profiles of fluo-

rescent dextran encapsulants of 4.4, 66, or 160 kDa, dissolved in sucrose. In any given vesicle, it is possible to monitor two labeled dextrans, in addition to sucrose, at the same time by using different fluorophores (e.g. fluorescein or rhodamine).

Fig. 4 illustrates the molecular weight dependence of encapsulant release. At initial times ($t=0$ h), the entire vesicle population (90–100%) retains all of its encapsulants (i.e. sucrose, 4.4 and 66 kDa dextran). By $t=18$ h, 22% of this vesicle population loses its sucrose. Within this set, nearly two-thirds (15% total) of the vesicles release the 4.4 kDa dextran and the remaining third (7%) lose all three of the encapsulants. This data (Fig. 4B) indicates that sucrose and the 4.4 kDa FITC-dextrans are released with respective $\tau_{release}$=66 and 89 h. In contrast, larger molecular weight dextrans (60 kDa) show little to no release from these same carriers until eventual vesicle disintegration occurs on the order of days.

To attribute a mean length-scale to the transient pore that develops in a vesicle membrane, encapsulant molecular weights were converted [65,66] to mean radii of gyration (R_g) with sucrose (0.34 kDa) and dextrans of 4.4, 60, and 160 kDa having respective R_g's of 0.9, 1.4, 4.8, and 7.3 nm. Given the vesicle leakage of all but the last dextran, a conservative upper bound of the hydrophilic pore size is estimated to be 5 nm. This mean radius corresponds to an initial pore diameter of ~ 10 nm, which is comparable to the cited membrane thickness of $d_{OL1} \sim 10.4$ nm (Fig. 1B) as well as $d_{OB18} \sim 15$ nm [39]. Whether or not there is an energetic basis for initial pore size is, at present, unclear.

As a more physical demonstration of carrier instability, the mechanical integrity of blended polymersome vesicles was tested by micropipette aspiration (not shown). Aspiration of an encapsulant loaded vesicle yields rupture strains of the same order of magnitude as pure OB18 vesicles [39]. In marked contrast, the phase light or empty polymersomes collapse readily under application of minimal aspiration pressures.

3.5. 100 nm-sized polymersome disintegration kinetics

Subsequent to poration, growth of membrane pores increasingly destabilizes the vesicle carrier
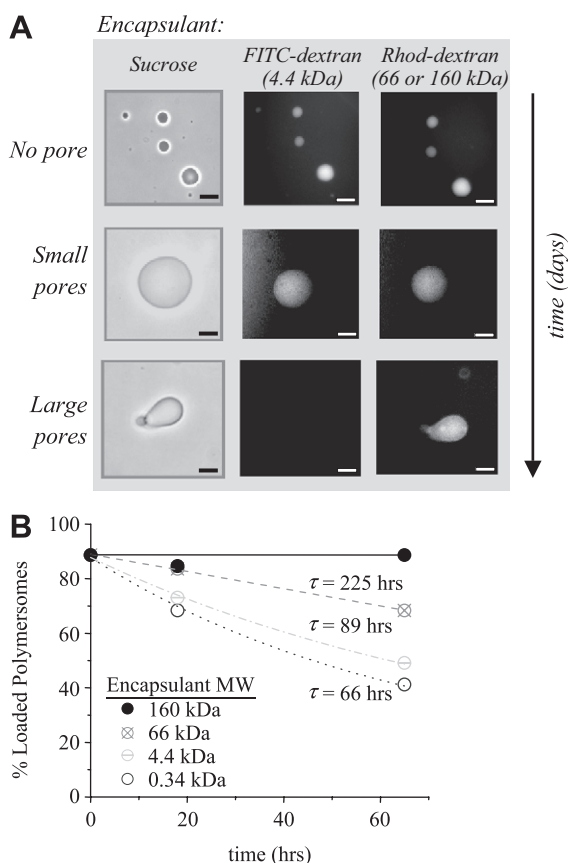
A *Encapsulant:*

B

Fig. 4. Phase contrast and fluorescent imaged kinetics of release from giant OL1/OB18 (25:75 mol%) vesicles loaded with a molecular weight series of dextrans in sucrose. (A) Sucrose and the FITC-dextran (4.4 kDa) are increasingly released over the 3-day duration of the experiment; but the large dextran (160 kDa) showed no release and thus provides an upper limit to a finite pore size in the membrane. Scale bars are 5 μm. (B) The indicated release time constants are determined from kinetics.

(Fig. 3A(iii)). To gain further insight into the complete loss of membrane integrity (especially with circulation-favored 100-nm vesicles [31]), dynamic light scattering (DLS) was used to monitor 100-nm vesicle populations of either OL1 or OL2 (Table 1: f_{EO}=0.49) again blended with OB18 (at 25:75 mole ratio as above). Vesicles were first sized down to a single population of 100 ± 20 nm by sonication, freeze thaw, and cyclic extrusion [64]. As a control, the scattering intensity of a pure OB18 vesicle population is found to remain constant throughout the course of the studies. However, the OL blends
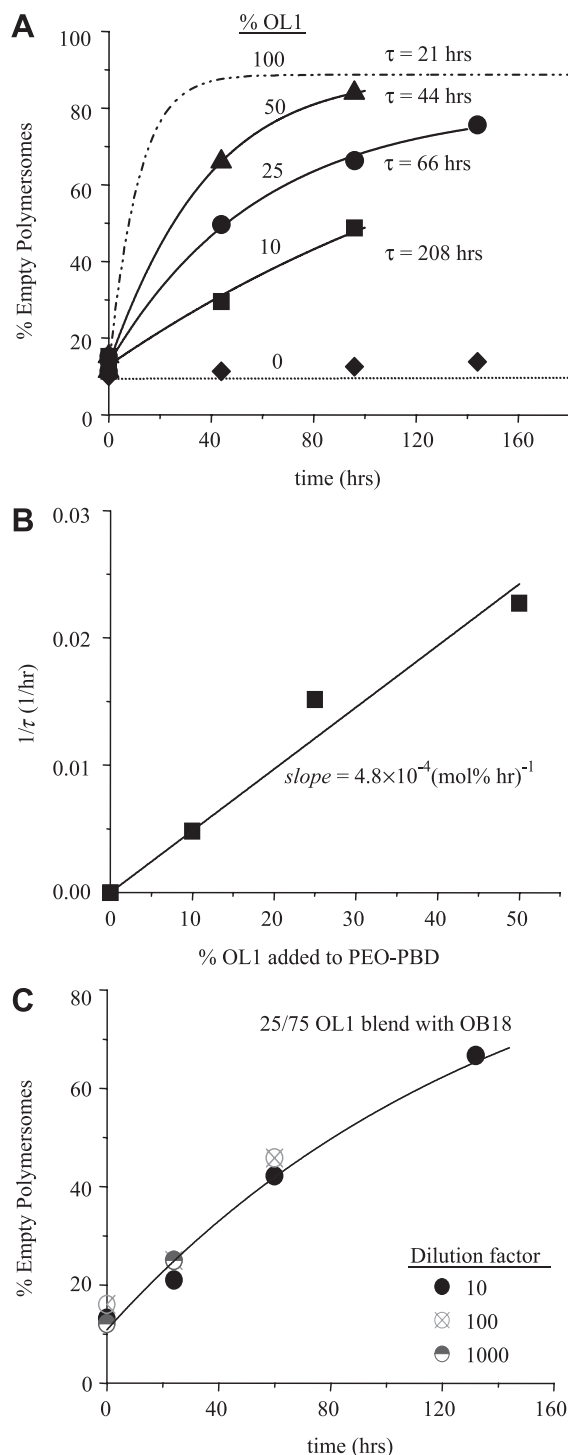
show a progressive decay in intensity of the 100-nm peak. This peak increasingly splits up into two distinct populations consisting of larger fragments of aggregates (perhaps extended vesicles or worms; see Fig. 1), and a smaller peak at 40 nm that probably corresponds to micelles. The latter identification is certainly consistent with prior characterizations of PEG–PLA micelles [45,46,49,67].

From DLS, disintegration time constants for the OL1 and OL2 blended vesicles were measured to be $\tau_{disintegration}$=12 and 4 days, respectively. The $\tau_{disintegration}$ for OL1 appeared to be several-fold longer than the $\tau_{release}$ determined for the same OL composition. The DLS results are therefore consistent with post-release disintegration. It might seem surprising that similar blends with OL2 display three-fold faster vesicle disintegration kinetics than OL1, especially since OL2's PLA block is less than one-fourth larger in molecular weight than OL1's (M_n; Table 1). However, the three-fold faster disintegration together with the concomitant emergence of a micelle peak implies that the larger a diblock's f_{EO} (as in OL2), the stronger its propensity to rapidly transform into a detergent-like moiety that tends to destabilize existing bilayer morphologies.

3.6. Blend-dependent release kinetics

The influence of hydrolysable PEG–PLA chains on release kinetics was further elucidated and directly controlled by varying the mole fraction of OL1 blended into the OB18 membrane. At initial times, nearly all vesicles (90–100%) were loaded with hydrophilic encapsulant, irrespective of blend ratio. Depending on this ratio, the characteristic release time ($\tau_{release}$) was observed to vary from tens of hours to days (Fig. 5): this figure indicates that an increasing mole fraction of OL1 in the aggregate system accelerates encapsulant release from these giant carriers (Fig. 3: i→ii, iii).

Monitoring vesicle populations in a blend for $t > \tau_{release}$ reveals a progressive disintegration of empty vesicles (see Fig. 3A(iii)). Loss of these empty vesicles results in an anomalous shift in the release curve and leads to an increase in the relative population of residual, "loaded" vesicles. Nonetheless, based on the initial observation times, the rate constant for release $k_{release}$=1/$\tau_{release}$ is found to be a linear

Fig. 5. Blend-controlled release kinetics of a small encapsulant from various polymer vesicle formulations. (A) Pure OB18 vesicles (0% OL1) porate minimally over time, but poration probability increases as a function of the mole percent of OL1 blended with OB18. The solid lines for 10%, 25%, and 50% blends are fits to $A[1-\exp{(t/\tau)}]$ with the indicated release times, $t=\tau_{release}$; and the dashed line is the extrapolated kinetics for 100% OL1 vesicles. (B) Plotting release kinetics $(1/\tau)$ vs. the mole percent of OL1 blended into the membranes shows a first-order rate dependence. (C) Release kinetics from 25 mol% blends monitored with various bulk dilutions into PBS. Subsequent, pore induction and deviations in the encapsulant release times are within 15% and therefore independent of dilution and exterior factors. In all of the experiments, the vesicles are suspended in buffered PBS (300 mosM) and incubated in closed chambers at 25 °C.

function of the initial mole percent of OL1 blended with inert OB18 (Fig. 5B):

$$k_{release} = const \times [polyester]_{\circ} \qquad (1)$$

Extrapolation of the plotted release kinetics to vesicles of pure (100%) OL1 (e.g. Fig. 1B) gives $\tau_{release} \sim 21$ h as sketched in Fig. 5A. This time scale is short relative to vesicle formation times of $\tau_{formation} \sim 10-15$ h. It is therefore clear why formation of pure PEG–polyester vesicle systems has remained elusive. Furthermore, these blends clearly deepen the understanding of the degradation process by protracting the release time scales. Indeed, robust characterizations of the lower mole fraction systems are not problematic since $\tau_{release} \gg \tau_{formation}$.

In an effort to concomitantly infer localization of PEG–PLA in the polymersome membrane as well as its role in facilitating encapsulant loss, release kinetics from 25:75 (mol%) blends was monitored after dilution, by up to three orders in magnitude of bulk solution. Fig. 5C demonstrates only minor deviations in the time scale of encapsulant release with such dilution ($\tau_{release} \pm 15\%$). Any bulk PEG–PLA must therefore have no role in the process. This confirms the central importance of polyester chains pre-localized in the vesicle membrane (per Fig. 1C) in both encapsulant release and eventual carrier destabilization. It is thus readily envisioned that for any individual vesicle, release is a burst-like, two-state process (Fig. 3). For a population of vesicles, this effect appears graded, as expected of a protracted first order process typified by Eq. (1). Lastly, as with the studies shown here using physiological buffer, initial tests of

vesicle poration in human plasma (and 37 °C) show similar initial stability and release profiles.

3.7. Release kinetics for PEG–PCL

To confirm a very general role for polyester hydrolysis as the 'trigger' for polymersome destabilization, the diblock copolymers of PEG–PCL (OCL's in Table 1) were also investigated. PCL, like PLA, is widely explored as a degradable polyester [19,20,68], but its six-carbon backbone makes it more hydrophobic than a PLA chain of comparable MW. When hydrated as pure diblocks, the OCL copolymers self-assemble into morphologies consistent with their respective f_{EO} fractions (see Table 1). For example, being near the phase boundary, OCL1 self-assembles into a mixed population of both vesicles and cylindrical or worm micelles. It is therefore not surprising that membrane blends with OCL's and the inert OB18 form just as readily as with the OL diblocks.

With 25:75 molar blends of OCL in OB18, encapsulant release kinetics from micron-sized vesicles are again a function of copolymer chemistry. OCL1 as well as both OL's (OL1 and OL2) have comparable hydrophobic block molecular weight (M_h=3.3±0.6 kDa). However, OCL1 has an intermediate f_{EO} (see Table 1). Therefore, one might naively expect OCL1-based vesicles to release faster than similar OL1 blended vesicle compositions. At the same time, OCL1-based vesicles should also release slower than blended compositions with OL2 ($\tau_{release}$=40 h; Table 2). Surprising perhaps, the release time determined for OCL1 ($\tau_{release}$=73 h) proves to be slightly longer than that of OL1 ($\tau_{release}$=66 h). This deviation from naïve expec-

tation provides the clearest indication of a slower hydrolysis for the more hydrophobic PCL chemistry within the membrane core.

The second PEG–PCL diblock, OCL2, has the most membrane-preferring proportions with f_{EO}=0.28. OCL2 also has a four-fold larger PCL block ($M_h \approx 13$ kDa). Encapsulant release from OCL2/OB18 vesicles proves to be two-fold slower in comparison with the most similarly proportioned OL1 ($f_{EO} \sim 0.33$) blends. One likely factor is that water activity in the PCL core is lower than in a PLA core. In addition, a greater degree of ester hydrolysis would be required to drive this stable bilayer-forming copolymer ($f_{EO} \sim 0.28$) into an active detergent-like molecule (f_{EO}>0.4) that then destabilizes the carrier membrane. Compared to molecular weight effects, both f_{EO} and polyester chemistry (PCL vs. PLA) thus play a more dominant role in dictating release kinetics.

4. Discussion

4.1. Copolymer integration into membranes

When hydrated initially, the PEG–polyester copolymers and blends self-assemble into stable bilayer architectures (e.g. Fig. 1B). The core thickness of the PLA membrane is similar to a previously studied PEG–PBD vesicle [39], namely EO_{50}-BD_{55} (with $d \approx 10.6 \pm 1$ nm). This OL1 result fits the general scaling found for PBD cores of $d \sim N^{0.5}$. While this may seem surprising because of PLA's high oxygen content, it is to be noted that such high oxygen contents in hydrophobic blocks are of no limitation to membrane formation. At least one Pluronic triblock copolymer with an oxygen-rich midblock (EO–polypropyleneoxide–EO) has previously been reported to form vesicles [69].

Membrane-localized fluorescent PLA demonstrates PEG–PLA integration (Fig. 1C). Further detailed intensity analysis of these labeled blends (Fig. 2) shows a strong linear trend as a function of the mol% added to the membrane. This proportional increase in fluorescent intensity along with NMR spectroscopy on 50:50 blends clearly shows membrane miscibility of OL in PEO–PBD. Separate evidence of mixing in blends has recently been demonstrated by free radical cross-linking of the

Table 2
Encapsulant release times or rates from pure or blended membranes with hyrolysable block copolymers

Copolymer name	$\tau_{release}$ (h) for 25:75 blend with OB18	$k_{release}$ ($\times 10^4$) (mol% in OB18 hr)$^{-1}$	$\tau_{release}$ (h) for pure copolymer[a]
OL1	67	4.7	22
OL2	40	10.1	0[b] (10)
OCL1	73	5.5	0[b] (18)
OCL2	129	3.1	32

[a] $\tau_{release}$ linearly extrapolated from 25% copolymer blends.

[b] $\tau_{release}$=0 for copolymers that cannot, when pure, form vesicles.

unsaturated polybutadiene (PBD) double bonds in OB18 [29]. Cross-linking effectively blocks lateral mobility of the PBD chains in the bilayer architecture. Extraction of the blended OL1 chains by chloroform leads to rapid encapsulant release (in minutes) and the consequential loss of membrane integrity. In contrast, cross-linked shells of pure OB18 prove extremely robust and unaffected by external chemical and physical stresses [70].

4.2. Release kinetics of hydrophilic encapsulants

Much of the previous work on PEG–PLA based aggregates can be categorized as assemblies of copolymers with low f_{EO} and large molecular weight PLA blocks, (a "crew-cut" presentation of PEG per Eisenberg et al. [23]), or else copolymers with $f_{EO}>0.4$. Depending on the nature of aggregate processing, the former generally leads to the sequestering of glassy, immobile PLA blocks into solid-like particles, whereas the latter leads to an assembly of micellar structures as per Fig. 1. Only lipophilic compounds can be intercalated into such diblock morphologies. Micellar aggregates give release profiles that correlate with progressive PLA degradation on the order of weeks [22,44] to months [71]. Particulate systems, on the other hand, display distinct biphasic burst profiles with repartitioning and leakage of a lipophilic drug varying from minutes to tens of hours [21,26]. A critical issue with PEG–PLA delivery systems is burst [22,26,72] vs. progressive degradation [44] release profile. Efforts have been made to suppress or rather "soften" this burst release by coating aggregates with proteins, amphiphiles, or polymers such as albumin [73], poloxamers [74], or detergents [22]. Here membrane blends of an inert copolymer plus PEG–PLA have succeeded not only in self-assembling into stable vesicles for hydrophilic encapsulant release but also in providing uniquely tunable release times ($\tau_{release}$=hours to days) that depend linearly on the blend ratio of PEG–PLA.

Additionally, the lack of dependence of $\tau_{release}$ on dilution of the vesicles (Fig. 5C) excludes any possible role of external copolymer (i.e. OL1) in vesicle poration. However, it could be hypothesized that OL1-mediated release is a result of OL1 polymer chains encapsulated within the lumen of inert OB18

vesicles. Such a mechanism can be dismissed on the basis that after vesicle poration, any encapsulated copolymer (being smaller than ∼10 nm) would be diluted into the bulk medium (see Fig. 4).

Polymer vesicles change shape by swelling and shrinking osmotically [30], which indicates that water permeates the core of the membrane. Such water can also initiate hydrolytic cleavage of the PLA or PCL blocks sequestered within the core. Considerable work has already been done on the mechanism of this water-initiated reaction [75], and it is well understood that the degradation of large molecular weight PLA blocks, self-assembled as either micelle or nanoparticles, takes on the order of months [21]. However, the presence of hydrophilic PEG, either through attachment [76,77] or blending [78] is claimed to direct the uptake of water, leading to accelerated (15-fold) dissolution kinetics [79].

4.3. Hydrolysis-driven membrane poration

The general mechanism of poration by PLA or PCL hydrolysis in the diblock copolymer membrane was illustrated in Fig. 6. The aqueous water microenvironment facilitates ester hydrolysis either by chain-end [15,76] and/or random [15,80] scission in the core of the membrane or perhaps at the PEG–polyester interface. If the latter interfacial degradation were dominant, the intact polyester block would simply
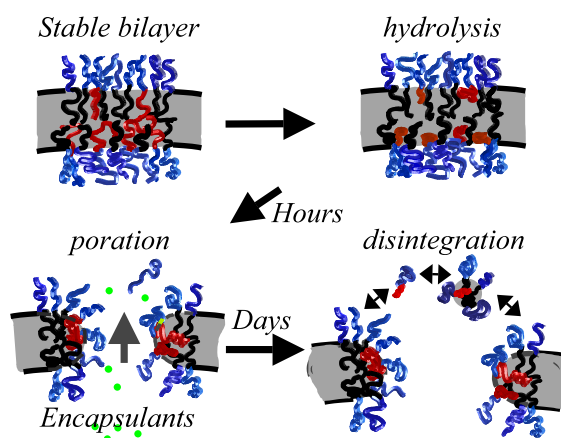

Fig. 6. Polyester trigger of encapsulant release and disintegration of polymersome vesicles. Red chains are degradable polyesters, and black chains are inert.

sequester within the richly hydrophobic core of the membrane, and create inclusions (not seen) while PEG diffuses away. In contrast, other mechanisms of PEG–polyester degradation eventually porate the vesicles.

The time constant found for characteristic release from 50:50 blends with OL1/OB18 ($\tau_{release}$=44 h) has been shown, with particles composed of similar PEO–PLA blocks ($f_{EO} \sim 0.33$), to liberate $\sim 50\%$ of the lactic acid [26]. Langer et al. [81] also studied similar particles and observed analogous release kinetics within an hour but with essentially $\sim 0\%$ lactic acid generation. These previous experiments imply that only a *small* fraction of the blended polyesters here is required to trigger the controlled destabilization of the vesicle carriers, consistent with Fig. 6.

The onset of hydrolysis and resultant curvature preference of OL1 chains in the membrane of a vesicle transforms this stable bilayer-forming chain into a detergent-like copolymer. Such degraded chains with comparatively short hydrophobic blocks will tend to segregate from their inert, entangled OB18 neighbors [64], congregate and perturb local bilayer curvature, and ultimately induce hydrophilic (i.e. PEG-lined) pores in the membrane. These salient molecular scale transitions are evident in physical observations such as molecular weight-dependent encapsulant release from otherwise intact vesicle carriers (Fig. 4). Liposomal systems have applied similar principles such as doping non-reactive amphiphiles with reactive ones [82] to exploit molecular scale transitions from lamellar to ''non-bilayer'' forming chains [8,83] or to inverted hexagonal phases [51–53] in order to concomitantly trigger encapsulant release and carrier destabilization.

To further verify evolution of OL1 chains into detergent-like triggers, pure encapsulant loaded OB18 vesicles were incubated with exogenous OL1 block copolymer in the aqueous bulk solution. Over time, the surface active OL1 chains increase (inert) vesicle permeability, and trigger the release of hydrophilic encapsulants (data not shown). Though OL activity appears to be analogous to detergent-mediated solubilization of vesicle membrane, the dissolution kinetics were three orders of magnitude slower than TX-100 solubilization of micron-sized OB18 vesicles [84]. This delay in vesicle instability parallels work by Ladaviere et al. [85,86] on liposome

destabilization by amphiphilic macromolecules. At least two distinctions are noteworthy; first, liposomal assemblies invariably lack the dense 100% PEGylated ''hairy'' brush that deters adsorption and integration of factors that limit vesicle circulation times in vivo [31]. Second, the ability of amphiphilic polymers to modulate membrane properties is conditional on the hydrophobicity of the adsorbing polymer. In the present case, the oxygen-rich PLA block handicaps the polymer and renders it a weak but adequate solubilizer. In particular, partially degraded polyester chains are responsible for curvature—minimizing the membrane line tension around pores—while also leading to the slow growth of pores in the, otherwise, impenetrable membrane. However, the molecular weight-dependent release profiles of hydrophilic dextrans from polymersomes (see Fig. 4) indicate stable pore sizes that approximate the membrane's thickness. A natural curiosity arises as to whether or not amphiphilic polymers exhibit self-healing tendencies in vesicle pores. Steric hindrance due to chain repulsion arises with the hairy PEG brush that lines the pore in the bilayer membrane, thereby deterring membrane resealing. This apparent stability of the small pore requires a different explanation such as highly localized hydrolysis and nucleation of an increasing number of similar-sized pores—which require longer time scales to coalesce. Regardless, PEG–polyester chains in bilayer morphology are poised to act as time-evolving molecular triggers that modulate encapsulant release and subsequent vesicle disintegration.

4.4. Microphase basis for poration kinetics

The phase boundaries indicated in Fig. 1 provide a framework for graphically understanding encapsulant release times as a function of the key variable f_{EO}. Considering first the two PEG–PLA's that were studied (Fig. 7A), the small difference in M_h was neglected and a single line was drawn through the two data points for 25% blends. The f_{EO} intercept of this first line (gray star: polyester diblock $f_{EO} \approx 0.73$) indicates a blended OL/OB18 system (25:75) which would give instant release upon vesicle formation. A nearly parallel line was also sketched through the result for 100% OL1, but this second line intersected the $\tau_{release}$=0 axis at f_{EO}=0.42 (open star). This inter-
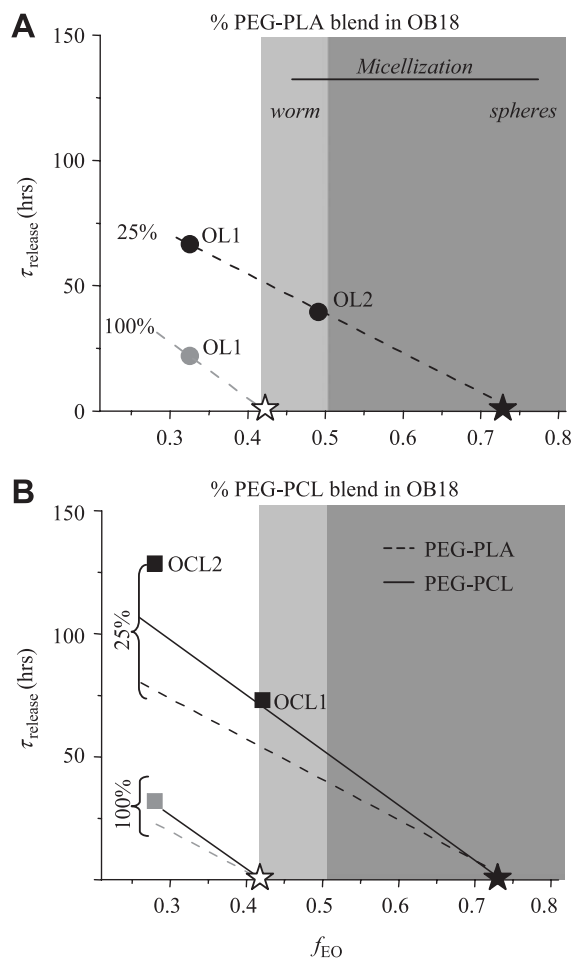
Fig. 7. Summary of encapsulant release kinetics from copolymer vesicles as dictated by both chain chemistry and PEG volume fraction (f_{EO}). (A) OL copolymers of several thousand g/mol can integrate at 25 mol% into stable vesicles of inert OB18 as long as $f_{EO} \leq 0.73$ (gray-filled star). For pure vesicles of such degradable copolymers (i.e. 100%), release is much faster and requires $f_{EO} \leq 0.42$ (open star). (B) OCL copolymer of similar M.W. to OL1 and OL2 degrades more slowly when accounted for the f_{EO} effects. This delay due to polyester chain chemistry reflects retarded PCL degradation kinetics. A characteristic release line through the result for the 25% OCL blend intersects the 25% OL line at $f_{EO}=0.73$, where f_{EO} dominates any major difference in degradation chemistry. Likewise, release from pure OCL vesicles can be predicted by postulating slower proportionate degradation but at a common microphase stability limit of $f_{EO}=0.42$. Comparing the two OCL1 lines to OCL2 data points reveals the M.W. effect or lack thereof since OCL2 is about four-fold bigger than OCL1 and the two OL block copolymers.

cept is again indicative of a system displaying instant release and dominant micelle formation as opposed to any significant vesicle-delayed encapsulant release. Similar conclusions were drawn from the PEG–PCL systems (at 25 mol%) plotted in Fig. 7B. While the baseline release from pure (100%) vesicles is theoretically important, both 'star' systems are impractical for release applications since high vesicle yields by standard hydration methods take a comparatively long formation time, as explained earlier.

Though the over-simplifications here do not fully address nuances of co-existence between vesicle/worm/sphere regimes found experimentally—such as those illustrated in Fig. 1B—the various lines on the two plots of Fig. 7 are assumed to be representative of release times for the three smaller block copolymers studied here (i.e. OL1, OL2, and OCL1). Lastly, for the larger OCL diblock, OCL2, the two square points off the lines in Fig. 7B highlight relatively small offsets (<25%), despite a ~4-fold larger hydrophobic block. Small offsets imply a minimal influence of M_h on release kinetics in comparison to the strong effects of a copolymer's initial f_{EO}. This conclusion is fully consistent with the assertion here that ±20% differences in M_h of the three smallest diblocks (i.e. OL1, OL2, OCL1: 3.3 ± 0.6 kDa) are simply insignificant to release kinetics.

Within the framework of microphase behavior, the moderate molecular weight polyester-based diblocks, such as the OL and OCL, self-assemble or integrate into bilayer architectures that are sensitized for release. Triggered by the initiation of hydrolysis in the core of the membrane, the onset of pores with highly curved edges leads to the observed release of lumenal encapsulants. Eventually, these vesicle carriers disintegrate into mixed micellar assemblies of worms and spheres. Polyester participation in the bilayer morphology appears to be strongly conditional on the rate of hydrolysis of the hydrophobic block (e.g. PCL vs. PLA) as well as the hydrophilic block ratio (f_{EO}). Another important means of controlling release involves the formation of blends of degradable polyesters with inert diblocks (e.g. $f_{EO}<0.73$ for 25:75 blends), and its stable integration into a mixed membrane. In contrast, for pure (100%) polyesters, extrapolations prove relatively independent of hydrophobic block chemistry and allow vesicle formation and release within $f_{EO}<0.42$.

5. Conclusions

The kinetics of hydrolytically triggered destabilization of polymersomes composed or blended with degradable PEG–PLA or PEG–PCL and the inert PEG–PBD (OB18) have been elucidated by sucrose and fluorophore leakage assays for giant vesicles as well as DLS of nanovesicles. Labeling of the PLA block demonstrates the participation of the polyester chain in stable membrane integration. Subsequent polyester hydrolysis in the core of the membrane transforms these bilayer-forming chains into active, detergent-like moieties that trigger the induction of pores in the vesicle membrane. Leakage of hydrophilic encapsulants occurs in a first-order, degradation-dependent fashion on time scales ranging from hours to tens of days. Molecular-weight-dependent encapsulant release assays determine the finite pore size to be comparable to the thickness of the vesicle membrane (~ 10 nm). Parallel studies with varied polyester hydrophilic/hydrophobic block ratios, hydrophobic core chemistry, and different mole percent blends indicates that polyester chain hydrolysis is the molecular trigger controlling encapsulant release and carrier destabilization kinetics.

Additional features of this potential drug delivery system include the 100% PEGylated brush that has been demonstrated elsewhere to effectively deter opsonization and prolong nano-sized vesicle circulation [31]. Polyester chains play a crucial role in conferring release mechanisms as well as definitive biocompatibility. Salient features of these polymersomes include resistance to destabilizing agents such as phospholipases and other lipid-disruptive components. The thick hydrophobic core of the vesicle membrane enhances loading efficiencies of lipophilic drugs. It should thus prove advantageous to study release and delivery of synergistically active lipophilic and hydrophilic drugs from these parent systems, since transitions from the bilayer to micellar regime may provide a sustained depot for lipophilic drug and impart novel pharmokinetics.

References

[1] D.D. Lasic, D. Papahadjopoulos, Medical Applications of Liposomes, Elsevier, Amsterdam, New York, 1998.

[2] D.X. Liu, F. Liu, Y.K. Song, Recognition and clearance of liposomes containing phosphatidylserine are mediated by serum opsonin, Biochimica et Biophysica Acta. Biomembranes 1235 (1995) 140–146.

[3] K. Jorgensen, J. Davidsen, O.G. Mouritsen, Biophysical mechanisms of phospholipase A2 activation and their use in liposome-based drug delivery, FEBS Letters 531 (2002) 23–27.

[4] J. Davidsen, K. Jorgensen, T.L. Andresen, O.G. Mouritsen, Secreted phospholipase A2 as a new trigger mechanism for localized liposomal drug release and absorption in diseased tissue, Biochimica et Biophysica Acta 1609 (2003) 95–101.

[5] O.V. Gerasimov, A. Schwan, D.H. Thompson, Acid-catalyzed plasmenylcholine hydrolysis and its effect on bilayer permeability: a quantitative study, Biochimica et Biophysica Acta 1324 (1997) 200–214.

[6] N.J. Wymer, O.V. Gerasimov, D.H. Thompson, Cascade liposomal triggering: Light-induced Ca+2 release from diplasmenylcholine liposomes triggers PLA2-catalyzed hydrolysis and contents leakage from DPPC liposomes, Bioconjugate Chemistry 9 (1998) 305–308.

[7] J.A. Boomer, D.H. Thompson, Synthesis of acid-labile diplasmenyl lipids for drug and gene delivery applications, Chemistry and Physics of Lipids 99 (1999) 145–153.

[8] G. Adlakha-Hutcheon, M.B. Bally, C.R. Shew, T.D. Madden, Controlled destabilization of a liposomal drug delivery system enhances mitoxantrone antitumor activity, Nature Biotechnology 17 (1999) 775–779.

[9] D. Kirpotin, K. Hong, N. Mullah, D. Papahadjopoulos, S. Zalipsky, Liposomes with detachable polymer coating: destabilization and fusion of dioleoylphosphatidylethanolamine vesicles triggered by cleavage of surface-grafted poly(ethylene glycol), FEBS Letters 388 (1996) 115–118.

[10] S. Zalipsky, M. Qazen, J.A. Walker, N. Mullah, Y.P. Quinn, S.K. Huang, New detachable poly(ethylene glycol) conjugates: cysteine-cleavable lipopolymers regenerating natural phospholipid, diacyl phosphatidylethanolamine, Bioconjugate Chemistry 10 (1999) 703–707.

[11] J. Shin, P. Shum, D.H. Thompson, Acid-triggered release via dePEGylation of DOPE liposomes containing acid-labile vinyl ether PEG–lipids, Journal of Controlled Release 91 (2003) 187–200.

[12] J.A. Boomer, H.D. Inerowicz, Z.-Y. Zhang, N. Bergstrand, K. Edwards, J.-M. Kim, D.H. Thompson, Acid-triggered release from sterically stabilized fusogenic liposomes via a hydrolytic dePEGylation strategy, Langmuir 19 (2003) 6408–6415.

[13] N. Bergstrand, M.C. Arfvidsson, J.-M. Kim, D.H. Thompson, K. Edwards, Interactions between pH-sensitive liposomes and model membranes, Biophysical Chemistry 104 (2003) 361–379.

[14] A.L. Klibanov, K. Maruyama, V.P. Torchilin, L. Huang, Amphipathic polyethyleneglycols effectively prolong the circulation times of liposomes, FEBS Letters 268 (1990) 235–237.

[15] A. Belbella, C. Vauthier, H. Fessi, J.P. Devissaguet, F. Puisieux, In vitro degradation of nanospheres from poly (D,L-lactides) of different molecular weights and polydispersities, International Journal of Pharmaceutics 129 (1996) 95–102.

[16] J.M. Anderson, M.S. Shive, Biodegradation and biocompatibility of PLA and PLGA microspheres, Advanced Drug Delivery Reviews 28 (1997) 5–24.

[17] A. Brunner, K. Mader, A. Gopfeich, pH and osmotic pressure inside biodegradable microspheres during erosion, Pharmaceutical Research 16 (1999) 847–853.

[18] B.H. Woo, J.W. Kostanski, S. Gebrekidan, B.A. Dani, B.C. Thanoo, P.P. DeLuca, Preparation, characterization and in vivo evaluation of 120-day poly(D,L-lactide) leuprolide microspheres, Journal of Controlled Release 75 (2001) 307–315.

[19] C.G. Pitt, Poly(e-caprolactone) and its copolymers, in: R. Langer, M. Chasin (Eds.), Biodegradable Polymers as Drug Delivery Systems, Marcel Dekker, New York, NY, 1990, pp. 71–120.

[20] J.S. Chawla, M.M. Amiji, Biodegradable poly(e-caprolactone) nanoparticles for tumor targeted delivery of tamoxifen, International Journal of Pharmaceutics 249 (2002) 127–138.

[21] R. Gref, Y. Minamitae, M.T. Peracchia, V. Trubetskoy, V. Torchillin, R. Langer, Biodegradable long-circulating polymeric nanospheres, Science 263 (1994) 1600–1603.

[22] J. Matsumoto, Y. Nakada, K. Sakurai, T. Nakamura, Y. Takahashi, Preparation of nanoparticles consisted of poly(L-lactide)–poly(ethylene glycol)–poly(L-lactide) and their evaluation in vitro, International Journal of Pharmaceutics 185 (1999) 93–101.

[23] C. Allen, J. Han, Y. Yu, D. Maysinger, A. Eisenberg, Poly-caprolactone-*b*-poly(ethylene oxide) copolymer micelles as a delivery vehicle for dihydrotestosterone, Journal of Controlled Release 63 (2000) 275–286.

[24] Z. Panagi, A. Beletsi, G. Evangelatos, E. Livaniou, D.S. Ithakissios, K. Avgoustakis, Effect of dose on the biodistribution and pharmacokinetics of PLGA and PLGA–mPEG nanoparticles, International Journal of Pharmaceutics 221 (2001) 143–152.

[25] T. Riley, S. Stolnik, C.R. Heald, C.D. Xiong, M.C. Garnett, L. Illum, S.S. Davis, S.C. Purkiss, R.J. Barlow, P.R. Gellert, Physicochemical evaluation of nanoparticles assembled from poly(lactic acid)–poly(ethylene glycol) (PLA–PEG) block copolymers as drug delivery vehicles, Langmuir 17 (2001) 3168–3174.

[26] K. Avgoustakis, A. Beletsi, Z. Panagi, P. Klepetsanis, A.G. Karydas, D.S. Ithakissios, PLGA–mPEG nanoparticles of cisplatin: in vivo nanoparticle degradation, in vitro drug release and in vivo drug residence in blood properties, Journal of Controlled Release 79 (2002) 123–135.

[27] D.E. Discher, A. Eisenberg, Polymer vesicles, Science 297 (2002) 967–973.

[28] F. Meng, C. Hiemstra, G.H.M. Engbers, J. Feijen, Biodegradable polymersomes, Macromolecules 36 (2003) 3004–3006.

[29] F. Ahmed, A. Popescu, D.E. Discher, B.M. Discher, Block copolymer assemblies with cross-link stabilization: from single component monolayers to bilayer blends with PEO–PLA, Langmuir 19 (2003) 6505–6511.

[30] B.M. Discher, Y.Y. Won, D.S. Ege, J.C.M. Lee, F.S. Bates, D.E. Discher, D.A. Hammer, Polymersomes: tough vesicles made from diblock copolymers, Science 284 (1999) 1143–1146.

[31] P.J. Photos, L. Bacakova, B.M. Discher, F.S. Bates, D.E. Discher, Polymer vesicles in vivo: correlations with PEG molecular weight, Journal of Controlled Release (2003) (in press, Available online).

[32] A. Kidane, T. McPherson, H.S. Shim, K. Park, Surface modification of polyethylene terephthalate using PEO–polybutadiene–PEO triblock copolymers, Colloids and Surfaces. B, Biointerfaces 18 (2000) 347–353.

[33] Y.C. Tseng, T. McPherson, C.S. Yuan, K. Park, Grafting of ethylene glycol-butadiene block copolymers onto dimethyldichlorosilane-coated glass by gamma-irradiation, Biomaterials 16 (1995) 963–972.

[34] F.S. Bates, Polymer–polymer phase behaviour, Science 251 (1991) 898–905.

[35] G.H. Fredrickson, F.S. Bates, Block copolymers—designer soft materials, Physics Today 52 (1999) 32–38.

[36] S. Jain, F.S. Bates, On the origins of morphological complexity in block copolymer surfactants, Science 300 (2003) 460–464.

[37] T. Govender, T. Riley, T. Ehtezazi, C. Garnett, S. Stolnik, L. Illum, S.S. Davis, Defining the drug incorporation properties of PLA–PEG nanoparticles, International Journal of Pharmaceutics 199 (2000) 95–110.

[38] C. Nardin, T. Hirt, J. Leukel, W. Meier, Polymerized ABA triblock copolymer vesicles, Langmuir 16 (2000) 1035–1041.

[39] H. Bermudez, A.K. Brannan, D.A. Hammer, F.S. Bates, D.E. Discher, Molecular weight dependence of polymersome membrane structure, elasticity, and stability, Macromolecules 35 (2002) 8203–8208.

[40] R. Dimova, U. Seifert, B. Pouligny, S. Forster, H.-G. Dobereiner, Hyperviscous diblock copolymer vesicles, European Physical Journal. E, Soft Matter 7 (2002) 241–250.

[41] F. Checot, S. Lecommandoux, H.-A. Klok, Y. Gnanou, From supramolecular polymersomes to stimuli-responsive nano-capsules based on poly(diene-*b*-peptide) diblock copolymers, European Physical Journal. E, Soft Matter 10 (2003) 25–35.

[42] F. Najafi, M.N. Sarbolouki, Biodegradable micelles/polymer-somes from fumeric/sebacic acids and poly(ethylene glycol), Biomaterials 24 (2003) 1175–1182.

[43] M. Valentini, A. Napoli, N. Tirelli, J.A. Hubbell, Precise determination of the hydrophilic/hydrophobic junction in polymeric vesicles, Langmuir 19 (2003) 4852–4855.

[44] E. Piskin, X. Kaitian, E.B. Denkbas, Z. Kucukyavuz, Novel PDLLA/PEG copolymer micelles as drug carriers, Journal of Biomaterials Science. Polymer Ed. 7 (1995) 359–373.

[45] K. Yasugi, T. Nakamura, Y. Nagasaki, M. Kato, K. Kataoka, Sugar-installed polymer micelles: synthesis and micellization of poly(ethylene glycol)−poly(D,L-lactide) block copolymers having sugar groups at the PEG chain end, Macromolecules 32 (1999) 8024–8032.

[46] H.K. Kim, T.G. Park, Surface stabilization of diblock PEG-PLGA micelles by polymerization of N-Vinyl-2-pyrrolidone, Macromolecular Rapid Communications 23 (2002) 26–31.

[47] Y.-Y. Won, H.T. Davis, F.S. Bates, Giant wormlike rubber micelles, Science 283 (1999) 960.

[48] P. Dalhaimer, F.S. Bates, H. Aranda-Espinoza, D.E. Discher, Synthetic cell elements from block coplolymers—hydrodynamic aspects, Comptes Rendus. Physique 4 (2003) 251–258.

[49] S.A. Hagan, A.G.A. Coombes, M.C. Garnett, S.E. Dunn, M.C. Davis, L. Illum, S.S. Davis, S.E. Harding, S. Purkiss, P.R. Gellert, Polylactide-poly(ethylene glycol) copolymers as drug delivery systems: 1. Characterization of water dispersible micelle-forming systems, Langmuir 12 (1996) 2153–2161.

[50] R. Savic, L. Luo, A. Eisenberg, D. Maysinger, Micellar nano-containers distribute to defined cytoplasmic organelles, Science 25 (2003) 615–618.

[51] J.W. Holland, P.R. Cullis, T.D. Madden, Poly(ethylene glycol)-lipid conjugates promote bilayer formation in mixtures of non-bilayer-forming lipids, Biochemistry 1996 (1996) 2610–2617.

[52] I.V. Zhigaltsev, N. Maurer, K.F. Wong, P.R. Cullis, Triggered release of doxorubicin following mixing of cationic and anionic liposomes, Biochimica et Biophysica Acta 1565 (2002) 129–135.

[53] X. Guo, A. MacKay, F.C. Szoka Jr., Mechanism of pH-triggered collapse of phosphatidylethanolamine liposomes stabilized by an ortho ester polyethyleneglycol lipid, Biophysical Journal 84 (2003) 1784–1795.

[54] M.A. Hillmyer, F.S. Bates, Synthesis and characterization of model polyalkane−poly(ethylene oxide) block copolymers, Macromolecules 29 (1996) 6994–7002.

[55] Z. Lin, M. He, L.E. Scriven, H.T. Davis, S.A. Snow, Vesicle formation in electrolyte solutions of a new cationic siloxane surfactant, Journal of Physical Chemistry 97 (1993) 3571.

[56] G. Haran, R. Cohen, L.K. Bar, Y. Barenholz, Transmembrane ammonium sulfate gradients in liposomes produce efficient and stable entrapment of amphipathic weak bases, Biochimica et Biophysica Acta 1151 (1993) 201–215.

[57] F. Arcamone, Doxorubicin: Anticancer Antibiotics, Academic Press, New York, 1981.

[58] G. Kong, G. Anyarambhatla, W.P. Petros, R.D. Braun, O.M. Colvin, D. Needham, M.W. Dewhirst, Efficacy of liposomes and hyperthermia in a human tumor xenograft model: im-portance of triggered drug release, Cancer Research 60 (2000) 6950–6957.

[59] K. Ulbrich, T. Etrych, P. Chytil, M. Jelinkova, B. Rihova, HPMA copolymer with pH-controlled release of doxorubicin—in vitro cytotoxicity and in vivo antitumor activity, Journal of Controlled Release 87 (2003) 33–47.

[60] J.S. Hrkach, M.T. Peracchia, A. Domb, N. Lotan, R. Langer, Nanotechnology for biomaterials engineering: structural characterization of amphiphilic polymeric nanoparticles by 1H NMR spectroscopy, Biomaterials 18 (1997) 27–30.

[61] A. Lucke, J. TeBmar, E. Schnell, G. Schmeer, A. Gopferich, Biodegradable poly(D,L-lactic acid)−poly(ethylene glycol)−monomethyl ether diblock copolymers: structures and surface properties relevant to their use as biomaterials, Biomaterials 21 (2000) 2361–2370.

[62] A.K. Salem, S.M. Cannizzaro, M.C. Davies, S.J.B. Tendler, C.J. Roberts, P.M. Wlliams, K.M. Shakesheff, Synthesis and characterization of a degradable poly(lactic acid)−polyethylene glycol copolymer with biotinylated end groups, Biomacromolecules 2 (2001) 575–580.

[63] H. Kukula, H. Schlaad, M. Antonietti, S. Forster, The formation of polymer vesicles or "peptosomes" by polybutadiene-block−poly(L-glutamate)s in dilute aqueous solution, Journal of the American Chemical Society 124 (2002) 1658–1663.

[64] J.C.M. Lee, H. Bermudez, B.M. Discher, M.A. Sheehan, Y.Y. Won, F.S. Bates, D.E. Discher, Preparation, stability, and in vitro performance of vesicles made with diblock copolymers, Biotechnology and Bioengineering 73 (2001) 135–145.

[65] Z. Bu, P.S. Russo, Diffusion of dextran in aqueous (Hydroxypropyl)cellulose, Macromolecules 27 (1994) 1187–1194.

[66] R.K. Hobbie, Transport through neutral membranes, Intermediate Physics for Medicine and Biology, 3rd ed., AIP Press, New York, 1997, pp. 114–124.

[67] J.H. Kim, K. Emoto, M. Iijima, Y. Nagasaki, T. Aoyagi, T. Okano, Y. Sakurai, K. Kataoka, Core-stabilized polymeric micelle as potential drug carrier: increased solubilization of taxol, Polymers for Advanced Technologies 10 (1999) 647–654.

[68] H. Kweon, M.K. Yoo, I.K. Park, T.H. Kim, H.C. Lee, J.S. Oh, T. Akaike, C.S. Cho, A novel degradable polycaprolactone networks for tissue engineering, Biomaterials 24 (2003) 801–808.

[69] K. Schillen, K. Bryskhe, Y.S. Mel'nikova, Vesicles formed from a poly(ethylene oxide)−poly(propylene oxide)−poly(ethylene oxide) triblock copolymer in dilute aqueous solution, Macromolecules 32 (1999) 6885–6888.

[70] B.M. Discher, H. Bermudez, D.A. Hammer, D.E. Discher, Y.Y. Won, F.S. Bates, Cross-linked polymersome membranes: vesicles with broadly adjustable properties, Journal of Physical Chemistry B 106 (2002) 2848–2854.

[71] J.W. Kostanski, B.C. Thanoo, P.P. DeLuca, Preparation, characterization, and in vitro evaluation of 1- and 4-month controlled release orntide PLA and PLGA microspheres, Pharmaceutical Development and Technology 5 (2000) 585–596.

[72] X. Li, X. Deng, Z. Huang, In vitro protein release and degradation of poly-DL-lactide−poly(ethylene glycol) microspheres with entrapped human serum albumin: quantitative evaluation

of the factors involved in protein release phases, Pharmaceutical Research 18 (2001) 117–124.

[73] H. Araki, T. Tani, M. Kodama, Antitumor effect of cisplatin incorporated into polylactic acid microcapsules, Artificial Organs 23 (1999) 161–168.

[74] T. Morita, Y. Horikiri, T. Suzuki, H. Yoshino, Applicability of various amphiphilic polymers to the modification of protein release kinetics from biodegradable reservoir-type microspheres, European Journal of Pharmaceutics and Biopharmaceutics 51 (2001) 45–53.

[75] E.A. Schmitt, D.R. Flanagan, R.J. Linhardt, Importance of distinct water environments in the hydrolysis of poly(DL-lactide-co-glycolide), Macromolecules 27 (1994) 743–748.

[76] S.S. Shah, K.J. Zhu, C.G. Pitt, Poly-DL-lactic acid: polyethylene glycol block copolymers. The influence of polyethylene glycol on the degradation of poly-DL-lactic acid, Journal of Biomaterials Science. Polymer Ed. 5 (1994) 421–431.

[77] X. Li, X. Deng, M. Yuan, C. Xiong, Z. Huang, Y. Zhang, W. Jia, In vitro degradation and release profiles of poly-DL-lactide–poly(ethylene glycol) microspheres with entrapped proteins, Journal of Applied Polymer Science 78 (2000) 140–148.

[78] W. Jiang, S.P. Schwendeman, Stabilization and controlled release of bovine serum albumin encapsulated in Poly(D,L-lactide) and Poly(ethylene glycol) microsphere blends, Pharmaceutical Research 18 (2001) 878–885.

[79] M. Penco, S. Marcioni, P. Ferruti, S. D' Antone, R. Deghenghi, Degradation behaviour of block copolymers containing poly(lactic–glycolic acid) and poly(ethylene glycol) segments, Biomaterials 17 (1996) 1583–1590.

[80] H.H.G. Jellinek, Aspects of Degradation and Stabilization of Polymers, Elsevier, New York, 1978.

[81] M.T. Peracchia, R. Gref, Y. Minamitae, A. Domb, N. Lotan, R. Langer, PEG-coated nanospheres from amphiphilic diblock and multiblock copolymers: investigation of their drug encapsulation and release characteristics, Journal of Controlled Release 46 (1997) 223–231.

[82] Y. Rui, S. Wang, P.S. Low, D.H. Thompson, Diplasmenylcholine–folate liposomes: an efficient vehicle for intracellular drug delivery, Journal of the American Chemical Society 120 (1998) 11213–11218.

[83] D. Needham, M.W. Dewhirst, The development and testing of a new temperature-sensitive drug delivery system for the treatment of solid tumors, Advanced Drug Delivery Reviews 53 (2001) 285–305.

[84] V. Pata, F. Ahmed, D.E. Discher, N. Dan, Detergent-mediated solubilization of polymersomes, Langmuir (2004) (submitted for publication).

[85] C. Ladaviere, M. Toustou, T. Gulik-Krzywicki, C. Tribet, Slow reorganization of small phosphatidylcholine vesicles upon adsorption of amphiphilic polymers, Journal of Colloid and Interface Science 241 (2001) 178–187.

[86] C. Ladaviere, C. Tribet, S. Cribier, Lateral organization of lipid membranes induced by amphiphilic polymer inclusions, Langmuir 18 (2002) 7320–7327.